

ARTICLES

Molecular Interactions in Thin Films of Hexadecafluorophthalocyaninatozinc (F₁₆PcZn) as Compared to Islands of *N,N'*-Dimethylperylene-3,4,9,10-biscarboximide (MePTCDI)**D. Schlettwein,* H. Graaf, J.-P. Meyer, T. Oekermann, and N. I. Jaeger***Institut für Angewandte und Physikalische Chemie, Universität Bremen, Postfach 33 04 40, D-28334 Bremen, Germany**Received: July 22, 1998; In Final Form: February 17, 1999*

Thin films (1–200 nm) of the title compounds were prepared by vapor deposition on glass at a controlled temperature. Film growth was studied in situ by optical absorption spectroscopy and measurement of the electrical conductivity. Independent of substrate temperature, a layered growth was found for ultrathin films of F₁₆PcZn. During further deposition, this was followed by island formation (Stranski–Krastanov). Island growth from the beginning of deposition (Volmer–Weber) was found for MePTCDI. Both growth modes were confirmed by atomic force microscopy (AFM). Substrate temperature had a clear influence on the crystal structure of F₁₆PcZn. A structure consisting of parallel stacks of molecules is formed first under all conditions. At lower temperature, this growth continues including, however, an increasing portion of amorphous material, whereas a square lattice of molecules is formed at higher temperature. This was found to be the stable modification of F₁₆PcZn since films deposited at lower temperature could be irreversibly transformed into this structure by annealing of the films. A reversible dependence of optical absorption spectra on temperature was found for the stable modification of both materials in the range from 78 to 450 K. Bands were found to narrow considerably at lower temperature, and shifts were observed that were characteristic for stronger intermolecular interaction which was very well-defined at lower temperature. A considerable mobility of molecules on the lattice site as well as between sites is indicated by the results of this study. The optical data are discussed in terms of an established model of transition dipole coupling.

Introduction

Thin films of crystalline organic materials have recently attracted quite some attention due to prospective applicability of their optical as well as electrical properties on one hand and due to their high versatility in film structure as influenced by molecular substituents, choice of substrate, and deposition conditions on the other hand.¹ Vapor deposition, if applicable to the molecules of interest, has proven to be one of the most reliable deposition technique to reproducibly obtain films of highest accessible quality.

In the past it has been shown that crystalline organic film growth can be obtained on crystalline as well as amorphous substrates.^{2,3} Among the most decisive deposition parameters was found the temperature of the substrate during deposition of the film. Different molecular orientations leading to different crystal structures were observed for phthalocyanines, e.g., phthalocyaninatofluoroaluminum(III) on SnS₂ (1000), as concluded from electron diffraction (RHEED) as well as optical absorption data.⁴ Also, after deposition annealing can lead to irreversible changes in the crystal structure of organic solids as long known from X-ray diffraction and optical absorption of phthalocyanine complexes of divalent metals.^{5,6} Such changes have been interpreted widely in terms of exciton dipole interaction leading to band splitting and selection rules which

could explain the obtained optical spectra as related to the structural analysis.^{7–12}

Irreversible as well as reversible changes with temperature have also been reported from optical emission studies of organic thin films. Emissions typical for monomeric 3,4,9,10-perylene-dianhydride (PTCDA) were detected for thin films on quartz glass at 10 K but disappeared at 100 K caused by excimer formation of PTCDA.¹³ Recently, monomer emission of PTCDA and *N,N'*-di-*n*-butylperylene-3,4,9,10-biscarboximide (C₄PTCDI) was detected at considerably higher temperature (up to 315 K) during the deposition of ultrathin films of about monolayer average thickness on freshly cleaved alkali halide (100) surfaces.¹⁴ The films showed changes on the time scale of a few minutes, indicating aggregation by a macroscopic mobility of the molecules on the surface as detected by an excimeric signal at longer wavelength typical for molecular aggregates/crystals which then showed a reversible temperature dependence as expected for excimer emissions indicating microscopic mobility of molecules on the lattice sites.¹⁵

The present study is aiming at a correlation between structure of organic films and optical as well as electrical characteristics. The contribution is focused on the influence of temperature on molecular mobility and changes in intermolecular interactions during thin film growth and during subsequent temperature changes as monitored by the optical absorption measured in situ and in transmission to obtain the highest precision and

* To whom correspondence should be addressed.

sensitivity. As a substrate, we chose resistively heated glass. Hexadecafluorophthalocyaninatozinc ($F_{16}PcZn$) represents the material of main interest in the present contribution as a representative of $F_{16}Pc$ which recently have attracted some attention due to their n-type character and an electron mobility that was found to be stable under ambient conditions.¹⁶ Different solid-state structures of $F_{16}PcZn$ were detected depending on temperature, and electrical as well as optical properties are discussed in terms of molecular interactions. These results obtained at $F_{16}PcZn$ are compared to those obtained at N,N' -dimethylperylene-3,4,9,10-biscarboximide (MePTCDI) as a representative of the perylene tetracarboxylic acid derivatives (PTCD). Opposite to phthalocyanines (Pc) polymorphism is generally not observed for PTCD. The materials grow without much distortion of their bulk structures on a variety of substrates. In the present paper, this is confirmed for MePTCDI despite a considerable mobility of the molecules on their lattice site as observed in the temperature dependence of the optical absorption.

Experimental Section

$F_{16}PcZn$ was synthesized as described earlier;¹⁷ MePTCDI was provided by Hoechst. Both materials were purified in a vacuum using a three-zone-sublimation apparatus from Lindberg.

As a substrate for film preparation we chose glass that was covered by ITO (indium tin oxide) on the backside of the sample. The ITO was used as a transparent resistive substrate heater. ITO films with a surface resistance of 50 Ω per square were the best choice for our experiments allowing temperature control between 273 and 478 K of the glass surface by easy control of heating voltage (up to 12 V) and current (up to 0.14 A). The maximum substrate temperature of 478 K could be reached by a heating power of only 1.7 W. In the visible spectra of this substrate, no change with temperature was detected during heating, only the UV absorption increased slightly due to changes in ITO absorption.

Thin film preparation took place in situ in a miniaturized vacuum chamber that was placed into a Varian Cary-4 spectrometer. That gave us the highest sensitivity and accuracy to measure optical properties of thin films intermittently (90° rotation of the substrate) during their deposition and without exposure to air. Custom-made vacuum fittings and chamber mounts were used to realize this geometry including two glass viewports (VAB Vakuumanlagenbau). For film deposition, sample materials were placed in resistively heated BN crucibles. The materials were deposited at sublimation rates ranging from 0.02 to 2 nm min⁻¹ as controlled by the resonance frequency of a 6 MHz quartz crystal microbalance. Using this setup, the films were prepared at 10⁻⁴ mbar (Balzers turbomolecular drag pump). The deposition source was placed rather close to the substrate (12 cm) due to geometrical restrictions in the spectrometer. During deposition the substrate temperature could therefore not be stabilized below about 318–338 K, dependent on temperature of the organic source. Higher substrate temperatures were obtained by resistive heating of the ITO on the backside of the substrate and controlled on the front by use of a K-type thermocouple. Samples deposited at about 30 °C were prepared on ITO at 10⁻⁵ mbar in a commercial bell jar vacuum system (CJT Vierkirchen). The sublimation rate was varied between 2.4 and 12 nm min⁻¹ as monitored by a commercial thickness monitor (Matex TM 100). Experiments at temperatures below room temperature were conducted at samples after transfer through air to a liquid N₂-cooled cryostat (Oxford

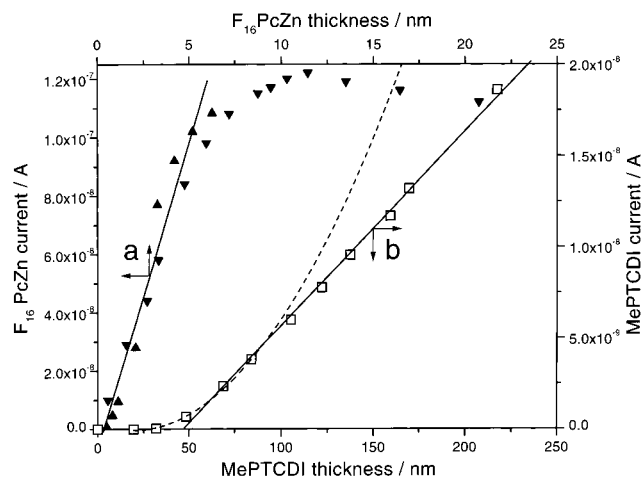


Figure 1. Changes in electrical conduction at an applied electrical field of 1 V cm⁻¹ as observed during deposition of $F_{16}PcZn$ (\blacktriangle , \blacktriangledown represent two sets of experiments) and MePTCDI (\square) on quartz glass at 430 K. The solid lines show linear increase, the dashed line shows a quadratic increase of current with film thickness.

Instruments Limited) which was placed in a Perkin-Elmer Lambda 9 spectrometer.

X-ray-diffraction was performed in a Bragg–Brentano X-ray diffractometer (Iso-Debye reflex 1001) using Cu K α radiation ($\lambda = 0.154$ nm) at 0.03° resolution for 10 min collection time at each angle. Film morphology was studied by atomic force microscopy in the tapping mode of a Nanoscope III system (Digital Instruments) using Si tips.

Results

Films were prepared and their electrical conductivity as well as optical absorption characteristics were studied beginning from about monolayer average coverage up to a macroscopic film thickness of about 100 nm. In situ electrical conductivity measurements and ex situ AFM analysis were carried out to establish the growth mode of films. Figure 1 shows measurements of the electrical conductivity as obtained during film growth of $F_{16}PcZn$ and MePTCDI at elevated temperature on quartz glass. A very different behavior was obtained for the two materials, pointing to the special characteristics of $F_{16}Pc$. During deposition of $F_{16}PcZn$, the current started to increase very sharply at less than 1 nm average film thickness (Figure 1a). Obviously conductive paths were formed already on a scale of monolayer coverage, indicating layered growth of $F_{16}PcZn$. This led to a nearly linear increase in the observed current until a film thickness of 5 nm was reached. From here on the further increase occurred at a decreasing slope until the current even decreased with increasing film thickness beginning at about 10 nm average coverage. Such a change would be characteristic for the formation of islands on top of the first layers (Stranski–Krastanov growth) which do not contribute to the current flow and which even grow at the expense of the first layers. For $F_{16}PcZn$ deposited at room temperature, we found a similar general dependence of current on the deposited amount with currents about 4 orders of magnitude lower. An improved crystallinity with increasing substrate temperature is thereby indicated. Islands of $F_{16}PcZn$ were already observed in AFM analysis of films as thin as 0.7 nm (Figure 2a). Flat portions in the image correspond to the thin layer which is initially formed and uncovered substrate.

For MePTCDI, typical island growth was obtained as also found earlier for phthalocyanine derivatives.¹⁸ Up to a thickness

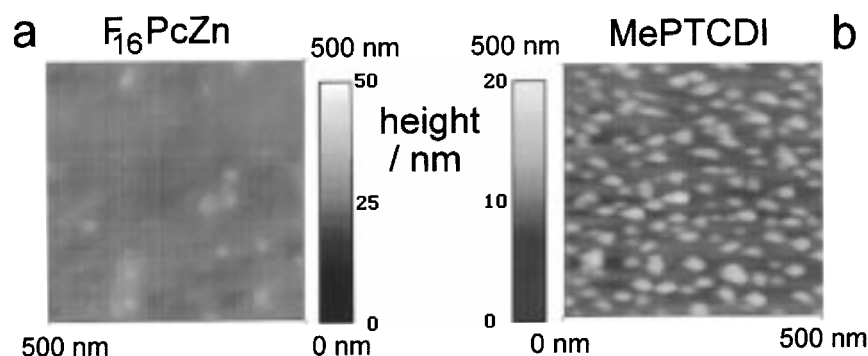


Figure 2. Morphology of 0.7 nm thin films ((a) $F_{16}PcZn$; (b) MePTCDI) deposited on quartz glass at 300 K as obtained from tapping mode AFM with a Si tip.

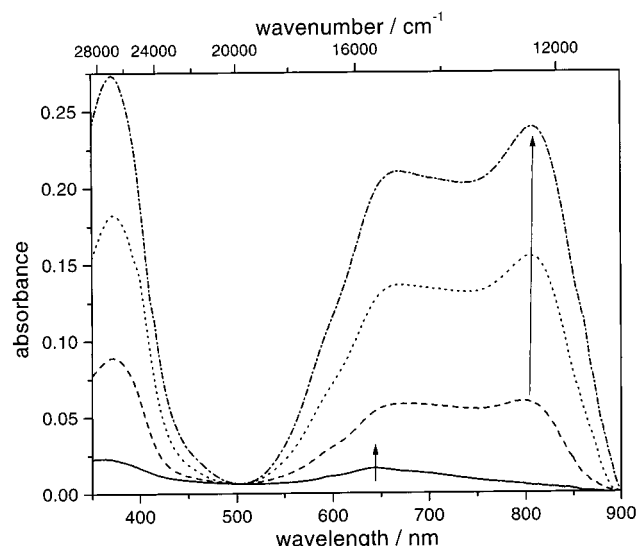


Figure 3. Optical absorption spectra during deposition of $F_{16}PcZn$ on glass at a substrate temperature of 453 K. Spectra are shown for a film thickness of 1 nm (—), 4 nm (---), 9 nm (---), and 16 nm (-.-). Arrows indicate dominating peaks.

of about 20 nm no increase of the current above the detection limit of about 10^{-14} A could be detected (Figure 1b). Thereafter the current increased due to the formation of conductive paths. Up to an average thickness of 80 nm, the number of conductive paths increased further characterized by a nearly quadratic increase of the current on film thickness as expected for paths formed by contact of islands. From here on the current increased in a linear way indicating three-dimensional growth of the bulk film. When this film was studied by use of an optical microscope, needles of up to 10 μ m length were seen. In a similar experiment performed during deposition of MePTCDI at room temperature, we observed the same growth mode, but the first conductive paths were observed at a significantly smaller average film thickness of only 10 nm indicating faster aggregation of MePTCDI with increasing substrate temperature. The morphology of the films in their initial state of growth was studied by AFM at films of about monolayer average coverage (about 0.7 nm) grown at room temperature on quartz glass (Figure 2b). Islands about 20–50 nm in diameter and about 10 nm in height were formed. The island growth mode of MePTCDI, as concluded above from conductivity measurements, was thereby directly confirmed also for thin films.

Optical spectra were collected in order to discuss the structural basis giving rise to the different growth modes observed. Depending on film thickness, substrate temperature during deposition, subsequent annealing temperature as well as sample

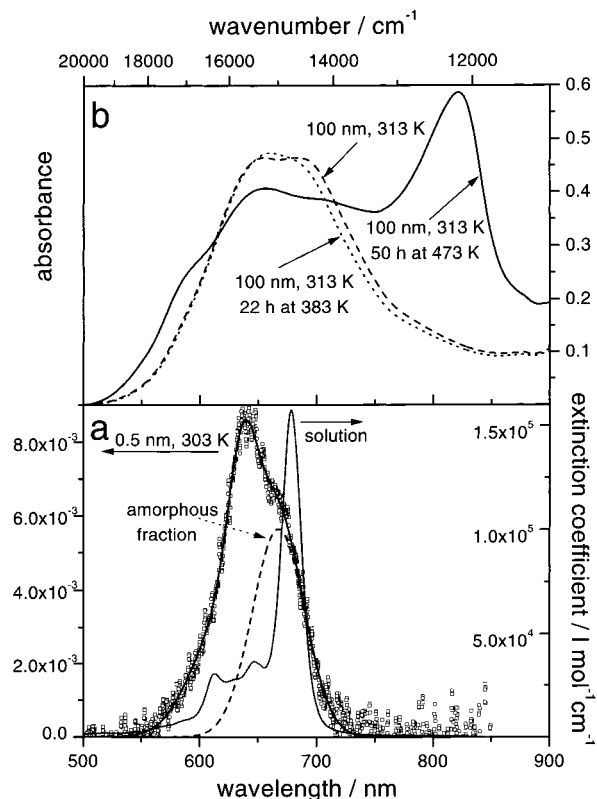


Figure 4. Optical absorption spectra measured at room temperature of (a) a 0.7 nm thin film of $F_{16}PcZn$ deposited on quartz glass of 303 K ($-\square-$, left axis) and of $F_{16}PcZn$ in pyridine solution (7×10^{-7} M, —, right axis). The dotted line (---) represents the amorphous portion of $F_{16}PcZn$ in the solid state (see text). (b) A 100 nm thin film deposited on ITO at 313 K (---) after annealing under ambient atmosphere at 383 K for 22 h (---) and after annealing at 473 K for 50 h (—).

temperature during spectra acquisition different molecular interactions were detected in situ in the optical spectra.

Figure 3 depicts a series of spectra as obtained during growth of $F_{16}PcZn$ on glass at elevated temperature. A single band at 640 nm ($15\,625\text{ cm}^{-1}$) was detected for the formation of the first monolayers (0.9 nm). This band dominated the spectrum before, at about 3 nm average thickness, a band at 820 nm ($12\,195\text{ cm}^{-1}$) increased to comparable height and dominated the spectrum of thicker films deposited at 453 K. This change of spectra clearly indicated two different kinds of intermolecular interactions and hence structures in the film when comparing the first monolayers to bulk films. As one band was blue-shifted by 876 cm^{-1} from the monomer absorption (Figure 4a) at 678 nm ($14\,749\text{ cm}^{-1}$) and the other was red-shifted by 2554 cm^{-1} , these changes in intermolecular interactions with film thickness seemed to be quite substantial. Differences observed between

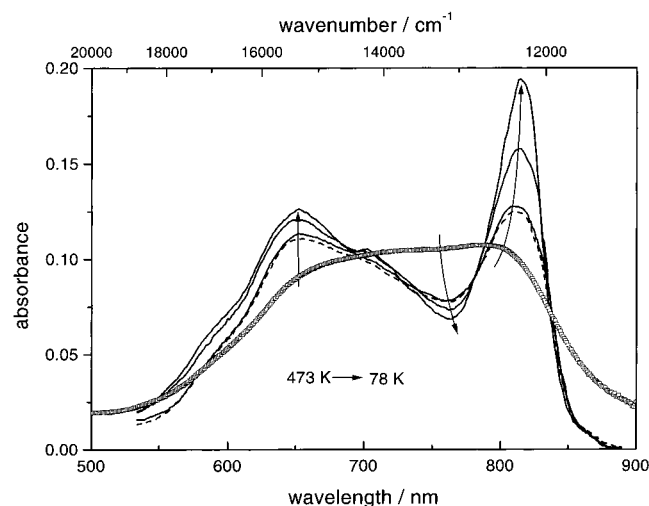


Figure 5. Temperature dependence of a 20 nm thin film deposited at 453 K on glass. Spectra are depicted at 298 K at the beginning of the experiment (---) and at the end (—), at 118 and 78 K. Open squares (□) represent the spectrum of a 30 nm thin film deposited at 453 K on glass measured during annealing in a vacuum at 473 K. Arrows indicate changes as observed with decreasing temperature.

films grown at 336 and 453 K did not exceed those observed in terms of the reversible temperature dependence as discussed below.

Films of $F_{16}PcZn$ showed a strong influence of substrate temperature on film structure. Intermolecular interactions in thin films and hence their crystallinity as detected by optical absorption and X-ray diffraction (XRD) of the thin films differed substantially. No influence of deposition rate was seen between 0.1 and 1 nm min⁻¹. In the larger vacuum system (ex situ analysis), films were prepared close to room temperature. Initially a very similar spectrum is obtained during deposition at 303 K substrate temperature (Figure 4a, 0.7 nm) when compared to 453 K (Figure 3, 1 nm). Clear differences were obtained in the spectra of thicker films deposited at 313 K (Figure 4b) compared to those at 453 K (Figure 3). The thin film of only a few monolayers average thickness deposited at 303 K (Figure 4a) showed a narrow absorption signal in the visible range at 645 nm which was fit by bands at 636 nm (15 723 cm⁻¹) and 667 nm (14 993 cm⁻¹). With increasing film thickness (not shown) the band at 667 nm shifted toward 672 nm (14 881 cm⁻¹) and broadened considerably. For thicker films of 100 nm (Figure 4b) two main bands became equally important and were observed at 654 nm (15 291 cm⁻¹) and 681 nm (14 684 cm⁻¹). The band at 820 nm was not found for films grown at 303 K. At 313 K, a small shoulder was seen at 820 nm (Figure 4b) but the peaks at 654 and 681 nm still clearly dominated the spectra.

Irreversible changes in absorption spectra could be observed for the films deposited at room temperature during subsequent heat treatment (Figure 4b). After 22 h at 383 K, the band at 681 nm decreased significantly in favor of the band at 654 nm with no change observable in the shoulder at 820 nm. Increasing the temperature to 473 K for 50 h led to a very characteristic change in the spectrum with the bands below 700 nm clearly decreased in intensity and the one at 820 nm in turn now being the dominant band in the spectrum. At 473 K $F_{16}PcZn$ already started to slowly sublime as seen in the proportional decrease of all bands in the spectrum after 70 more hours at this temperature (not shown). Heating the film above 473 K as performed for one of the films measured in situ led to a fast decrease of all peaks accompanied by a transient appearance

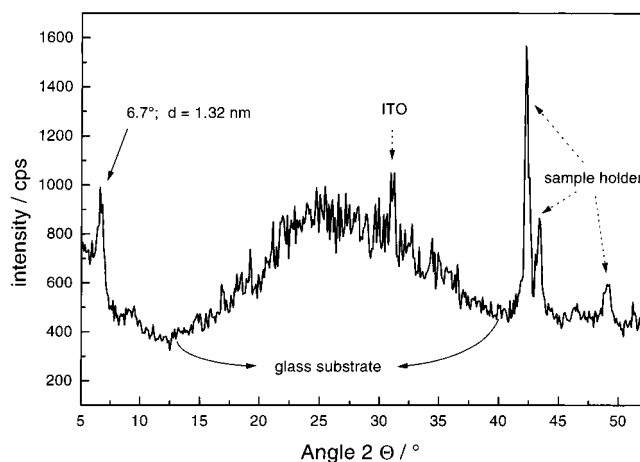


Figure 6. X-ray diffraction pattern as obtained from a 100 nm thin film of $F_{16}PcZn$ deposited at 313 K on ITO and annealed for 50 h at 473 K. Aside from the sample signal ($2\theta = 6.7^\circ$), peaks originating from the ITO substrate and from the sample holder are indicated.

of one broad signal (Figure 5, squares). If films were cooled to room temperature, however, similar spectra were obtained for films that were grown at room temperature and annealed at 473 K compared to those that were grown at 453 K. This comparison pointed toward a reversible dependence on temperature of this stable modification. Figure 5 further depicts the changes as observed at a film in this high-temperature modification in an extended range of temperatures by use of a cryostat that allowed measurements down to 78 K. All peaks in the spectrum became narrower at lower temperature and the peak at 820 nm red-shifted and increased in relative intensity to clearly dominate the spectrum, indicating a high degree of molecular order in the films (see below). These changes were fully reversible when the film was warmed.

The X-ray-diffraction measurements performed at films annealed at 453 K gave a diffraction signal at $2\theta = 6.7^\circ$ superimposed to a broad background originating from the glass substrate and ITO diffraction peaks (Figure 6). The angle corresponds to a distance of 1.32 nm. For the films grown at 313 K, we could obtain no distinct signals despite of comparable film thickness. A rather high crystallinity of the modification absorbing at 820 nm is thereby indicated.

Figure 7a depicts a series of spectra obtained during deposition of MePTCDI at 323 K. From the beginning of deposition, the spectra are characterized by two main branches, one blue shifted and one red shifted with respect to the 0–0 monomer absorption band in solution (depicted in Figure 7b). Only small differences in the fine structure in the spectra of the first deposited monolayers of MePTCDI as compared to a bulk film are observed; unlike the situation at $F_{16}PcZn$, the general band structure remains constant throughout the deposition. Up to 2 nm average thickness, the spectra were dominated by absorption bands at 466 nm (21 459 cm⁻¹), blue shifted by 2375 cm⁻¹ from the monomer, and at 538 nm (18 587 cm⁻¹), red shifted by 497 cm⁻¹. With increasing thickness the band at 572 nm (17 483 cm⁻¹), red shifted by 1601 cm⁻¹ from the monomer absorption, evolves. For films above 10 nm average thickness we found the main absorptions at 483 nm (20 576 cm⁻¹, blue shifted by 1492 cm⁻¹ from the monomer) and 572 nm (17 483 cm⁻¹). This situation already resembled the data obtained for a bulk film (200 nm) as reported in the literature¹⁹ characterized by absorptions at 486 and 574 nm. Different sublimation rates between 0.16 and 0.8 nm/min did not influence these optical characteristics of films during their growth.

Films deposited at 420 K, slightly below the sublimation temperature of MePTCDI (440 K), in principle showed the same behavior (not shown), but some fine structure was lost and the transition in the red-shifted branch was decreased in intensity and shifted by 182 cm^{-1} to higher energy. This change in characteristics relative to the films deposited at 323 K, however, was not permanent as the features observed at 323 K were also observed at the films deposited at this higher temperature when the temperature was lowered accordingly. Films deposited at 323 K also showed the same loss of fine structure when heated to 420 K. Temperature-induced changes observed at films of MePTCDI were therefore completely reversible and only dependent on the temperature during the optical measurement. In a subsequent series of experiments, optical spectra were measured in a larger range of sample temperatures (Figure 7b). When the films were cooled below room temperature the peaks as listed above changed in relative intensity and narrowed considerably allowing a better analysis of spectral fine structure. At 78 K, the peak most blue shifted, e.g., was passed in intensity by the red-shifted peak that was now shifted further to $17\,241\text{ cm}^{-1}$ (-1843 cm^{-1} relative to the monomer). When films were warmed to room temperature, all spectra changed reversibly to those observed earlier.

As a strong influence of oxygen exposure on the electrical properties of both materials¹⁸ and on the optical emission properties of PTCd had been observed,¹⁴ we also studied the influence of oxygen or air on the optical absorption characteristics. For both electrode materials, no influence could be observed independent of film thickness and deposition temperature.

Discussion

Different Growth Modes. The growth of F_{16}PcZn and MePTCDI films on quartz glass is discussed according to the different experiments spanning from macroscopic electrical properties (scale of millimeters) to film morphology (scale of micrometers) and intermolecular interaction (scale of nanometers). The Stranski–Krastanov growth mode of F_{16}PcZn as opposed to island growth of MePTCDI was inferred from the thickness dependence of the current measured during film growth (Figure 1) and was correlated to the intermolecular interaction as reflected in the visible absorption spectra (Figure 3; Figure 7a) obtained under comparable growth conditions.

In the case of F_{16}PcZn , interactions with the quartz substrate were strong enough to favor the formation of an initial layer of F_{16}PcZn . Such a growth mode had also been observed for F_{16}PcCu on SiO_2 lately and an orientation of the molecules perpendicular to the substrate was concluded from X-ray and electron diffraction.¹⁶ The large islands in the present experiments formed during subsequent deposition and their large distance from each other (Figure 2) indicate rather small intermolecular interactions of deposited molecules with the F_{16}PcZn layer which allow a high mobility of molecules on top of the layered portion. Within the islands, however, intermolecular stabilization seems to be considerably higher than within the initial layer since the islands are growing even at the expense of the first layers as seen from the decrease of the observed current despite a further increase of the average film thickness. X-ray analysis during a similar dependence found for PcCu led to the conclusion that an amorphous film of PcCu was formed first (which then had to be assigned to have a rather high specific conductivity) followed by crystallization of the film at higher average thickness which led to the observed decrease in conductivity.²⁰ Instead of this similarity of a decreasing current

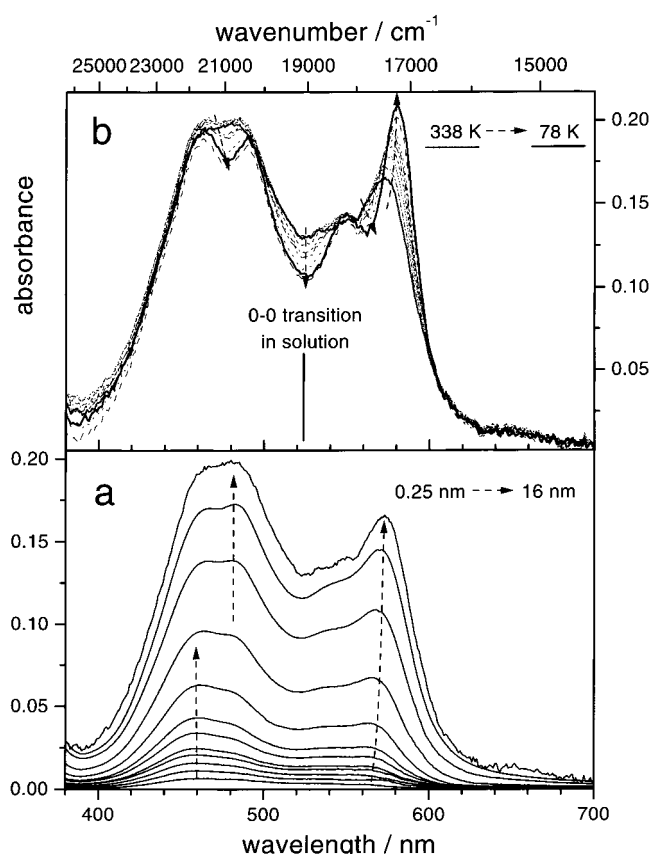


Figure 7. (a) Optical absorption spectra during deposition of MePTCDI on glass at a substrate temperature of 323 K. Spectra are shown for a film thickness of 0.25, 0.5, 0.75, 1.00, 1.25, 1.85, 2.50, 3.75, 6.25, 10.00, and 12.00 nm. Arrows indicate the most prominent spectral changes observed with increasing film thickness. (b) Optical absorption spectra during temperature variation at a 16 nm thin film of MePTCDI deposited at 323 K. Spectra are depicted for sample temperatures of 338 (—), 296, 278, 248, 218, 198, 178, 158, 118, and 78 K (—). Arrows indicate changes as observed with decreasing temperature. The vertical line represents the position of the lowest energy monomer absorption measured for $\text{C}_{16}\text{PTCDI}$ in CH_2Cl_2 solution.

with increasing average film thickness the present optical data indicate crystalline growth of F_{16}PcZn from the beginning of film growth as well as an amorphous fraction.

The structure of F_{16}PcZn strongly depended on the temperature during film deposition (Figure 4). By subsequent heat treatment, however, the same stable modification was reached after deposition on substrates of lower temperature as grown immediately under deposition onto warmer substrates. A remarkable mobility of F_{16}PcZn was indicated to allow such a ripening reaction.

MePTCDI showed a strong tendency toward island formation which was caused by thermodynamic stabilization of the islands, as the mobility of MePTCDI molecules on the substrate had to be quite high, concluded from the considerable distance and size of islands. A by far lower flexibility of MePTCDI intermolecular interactions in the solid state seems to be the origin of this difference compared to F_{16}PcZn . Changes in relative band height in the optical absorption spectra were indicative of only slightly different molecular orders in the initial growth stage as compared to the stable bulk structure which was established at an average film thickness between 6 and 12 nm (Figure 7a). First continuous contact of these crystalline islands across the 7 nm electrode distance was only detected after an average thickness of 20 nm (Figure 1b).

Both modes, island (MePTCDI) or Stranski–Krastanov

growth (F₁₆PcZn) finally led to island formation in the stable bulk crystal structure of the respective material.

Despite the strong differences in film growth and structural differences among the two samples, the temperature dependence of the optical absorption of the stable modification showed a very comparable reversible behavior in films of both materials. All bands sharpened considerably at lower temperature (Figure 5; Figure 7b). On the individual lattice sites both molecules seem to possess a quite high mobility even at liquid N₂ temperature, as indicated by the spectral changes which still could be observed at this temperature.

Chromophore Coupling. To discuss structural changes and their implication on film growth modes, the observed spectral changes and the underlying intermolecular interactions should be analyzed in more detail. Although changes in the intramolecular electronic structure²¹ as a consequence of intermolecular interactions could not be ruled out, dipole coupling of the optical excitations^{2,7–12,22,23} appears to be the most straightforward approach to explain the spectral changes. From X-ray studies at various Pc it was stated that molecular distortion was far less important at complexes of divalent central atoms as compared to tri- or tetravalent central metals carrying additional axial ligands.²¹ In analogy we assume that molecular distortions are of comparably small importance to discuss our present F₁₆PcZn data. For PTCDI to our knowledge no influence of molecular distortion on optical properties in crystals has been reported. Further, from optical as compared to X-ray structural analysis, the crystallochromic effects observed in a number of PTCDI could be explained by the relative orientation of molecules in the crystal.^{24–26} A quantum mechanical model has been used to further estimate the intermolecular electronic interactions in these crystals.²⁷ The high similarity of the present observations at these two very different molecular structures of F₁₆PcZn and MePTCDI further supports the approach of using a general model of intermolecular electronic coupling.

According to the model of transition dipole interaction, the energy of an ordered multilayer thin film is given by

$$\Delta E_{\text{CR}} = \Delta E_{\text{S}} + D - S + e \quad (1)$$

where ΔE_{CR} is the transition energy, ΔE_{S} is the energy of the transition for the molecule in solution, $D - S$ is the difference between the van der Waals intermolecular energies in the excited and the ground state as compared between the solid state and a solution, and $|e|$ is the sum of the coupling energies of the transition dipoles in the film.⁸ The value of $|e|$ strongly depends on the relative geometry of chromophores, but it is always proportional to the transition dipole moment $|M|^2$ and to r^{-3} , with r being the distance of dipole centers. $|M|^2$ is related to the dimensionless oscillator strength f of the transition which can be obtained from the integration of absorption spectra in solution.

$$f = \frac{8\pi m_e}{3h q_e^2} \nu g |M|^2 = \frac{4m_e c \epsilon_0 \ln 10}{N_A q_e^2} \int \epsilon \, d\nu \quad (2)$$

where ν is the transition frequency of the monomer in s⁻¹, g is the degeneracy of the excited state, $|M|^2$ is the dipole strength in C² m², ϵ is the molar extinction coefficient at the frequency ν , and the other symbols carry their usual meaning (m_e , mass of electron; h , Planck's constant; q_e , elemental charge; c , velocity of light; ϵ_0 , vacuum permittivity; N_A , Avogadro's constant). Using this relation, f and $|M|^2$ for both molecules of interest were determined from solution spectra and are listed in Table 1. The values for F₁₆PcZn were determined directly from

TABLE 1: Monomer Absorption Maximum, Oscillator Strength f , and Transition Dipole Moment $|M|^2$ As Determined from Integration of Solution Spectra of F₁₆PcZn in Pyridine and of C₁₆PTCDI in CH₂Cl₂

	absorption of the monomer/cm ⁻¹	oscillator strength f	transition dipole moment $ M ^2$ /C ² m ²
F ₁₆ PcZn	14 749 (678 nm)	0.59	4.72×10^{-58}
C ₁₆ PTCDI	19 084 (524 nm)	0.40	6.76×10^{-58}

integration of the solution spectrum, those relevant for MePTCDI were calculated from a spectrum of *N,N'*-dihexadecylperylene-3,4,9,10-biscarboximide (C₁₆PTCDI) and an extinction coefficient $\epsilon = 90\,000 \text{ L mol}^{-1} \text{ cm}^{-1}$ as reported in the literature²⁸ assuming a constant vibrational fine structure for PTCDI. C₁₆PTCDI was chosen to ensure sufficient solubility in order to measure a monomer spectrum since the alkane chain is known not to influence the transition energy of the PTCDI chromophore significantly.^{29,30} The value $|M|^2 = 4.72 \times 10^{-58} \text{ C}^2 \text{ m}^2$ ($= 4.24 \times 10^{-35} \text{ erg cm}^3$) as obtained for F₁₆PcZn falls into the range of values as reported for unsubstituted Pc (between 0.85×10^{-35} and $6.15 \times 10^{-35} \text{ erg cm}^3$)¹¹ and tetrapyrrodotetraazaporphyrins (2.56×10^{-35} and $2.68 \times 10^{-35} \text{ erg cm}^3$).¹² The value of $f = 0.4$ obtained for PTCDI also appears very reasonable compared to $f = 0.44$ as reported for perylene.³¹

Two limiting cases of dipole interaction geometry are of special interest to be discussed in eq 1: in a head-to-tail arrangement of transition dipoles, only negative values of e give allowed transitions (red shift of the band); in a parallel arrangement of the dipoles, only positive values of e give allowed transitions (blue shift of the band).¹⁰

Structure of F₁₆PcZn Thin Films. The present optical data indicate that the highly conductive thin film of F₁₆PcZn formed first during deposition predominantly consists of a rather well-defined molecular interaction geometry as the spectra of about 1 nm thin films (Figure 3; Figure 4a) are characterized by bands significantly blue shifted (925 and 969 cm⁻¹, respectively) relative to the monomer absorption in solution (14 749 cm⁻¹). Such a blue shift is typical for a parallel arrangement of chromophores and hence speaks for parallel stacks of F₁₆PcZn in this initial stage of growth, as also found in Pc films having strong axial interaction of the molecules.⁷ In our electrical experiments we found that these stacks of F₁₆PcZn formed a rather highly conductive layer. This can only be realized if the molecules were oriented nearly vertical to the substrate allowing strong π - π interaction in the plane of conduction. Such an arrangement of molecules had also been reported in films of F₁₆PcCu on SiO₂/Si leading to rather high field effect mobility of charge carriers.¹⁶ Stacks of F₁₆Pc with the molecules vertical to the substrate could be caused by the F atoms pointing outward, thus preventing strong interaction of the molecular π center with new arriving molecules and blocking island formation. Aside from these well-defined stacks, there is a shoulder in these thin film spectra (Figure 4a) rather close to the monomer absorption (blue shifted relative to the solution spectrum by 132 and 244 cm⁻¹, respectively) which we assign to molecules on the surface with no specific intermolecular electronic interaction (amorphous arrangement). The spectrum of 100 nm thin films deposited at room temperature showed a doublet of bands split from this amorphous band, indicating a rather small interaction of chromophores, probably accompanied still by an amorphous fraction (Figure 4b). Annealing this film for 22 h at 383 K increased this portion as only one band was detected close to the amorphous band. These defects were efficiently healed out, however, during annealing of the film at 473 K, and the

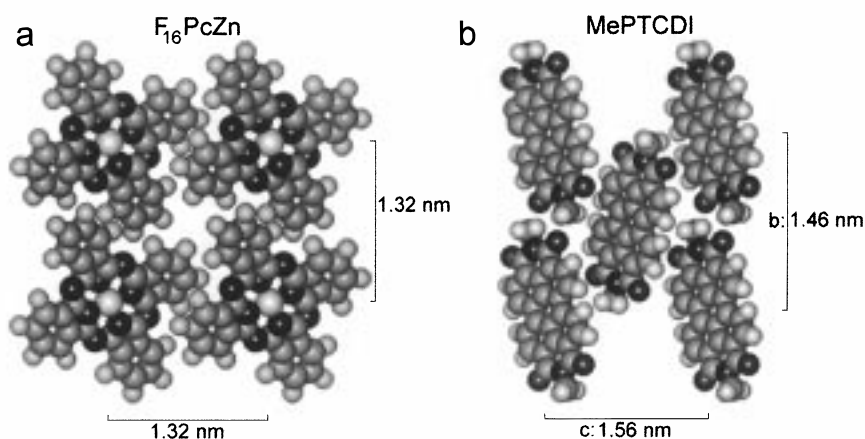


Figure 8. Space-filling model of $F_{16}PcZn$ as concluded from XRD and UV-vis analysis and of MePTCDI as reported in the Cambridge Structural Database.

formation of another crystalline modification characterized by the band strongly red shifted from the monomer transition (Figure 4b) was observed. X-ray diffraction peaks (Figure 6) could be obtained only for this modification with a lattice constant of 1.32 nm. This value is smaller than data from the literature. A signal at 6.1° corresponding to a distance of 1.42 nm for a sublimed powder sample of $F_{16}PcZn$, and at 6.4° corresponding to a distance of 1.38 nm for a 150 nm thin film on ITO also showing the red shifted band in the visible absorption were described earlier.³² For thin films of $F_{16}PcCu$ on SiO_2/Si an angle of 6.02° corresponding to 1.46 nm had been reported for an arrangement in parallel stacks of $F_{16}PcCu$.¹⁶ The large differences found for $F_{16}PcZn$ indicate a high degree of polycrystallinity as also concluded from our UV-vis absorption data. The distance of 1.32 nm (Figure 6) is consistent with the in-plane square lattice of $F_{16}PcZn$ as shown in the space-filling model in Figure 8a although it requires a rather dense packing. The geometry of the $F_{16}PcZn$ molecule was calculated by a molecular mechanics geometry optimization (mm⁺). The arrangement of molecules proposed would explain the strong red shift of the optical transition by 2554 cm^{-1} to 820 nm ($12\,195\text{ cm}^{-1}$) as arising from this planar in-plane lattice of molecules, with the molecules in the next layer shifted by half a lattice constant in the two directions of the square lattice.¹¹ Such an arrangement would lead to a position of the central metal of the adjacent layer right on top of the free space in the center of the square as often observed in crystalline Pc thin films.²

If the geometry of the model depicted in Figure 8a is used to calculate the dipole splitting energy e according to the equation

$$e = -11.06|M|^2/r^3 \quad (3)$$

as derived for this case¹¹ we obtain $e = -1050\text{ cm}^{-1}$. Using the shift of the amorphous band relative to the one in solution (Figure 4a), a value for $D - S = 188\text{ cm}^{-1}$ is estimated. It should be noted that this experimental value is positive (stabilization of the ground state relative to the excited state in the solid matrix compared to the solution) as opposed to the negative values experimentally determined for tetrapyrrodo-tetraazaporphyrine thin films ($D - S = -172\text{ cm}^{-1}$ for the zinc complex)¹² and to fit data from trivalent phthalocyanine thin films ($D - S = -175$ to -734 cm^{-1}).¹¹ The position of the resulting band is then obtained at 720 nm ($13\,887\text{ cm}^{-1}$). As the experimental result showed the position to be shifted to 820 nm ($12\,195\text{ cm}^{-1}$), either the molecules would have to be positioned even closer, which appears rather unlikely, or the vertical interaction of adjacent layers would have to be stronger

leading to a larger prefactor in eq 3 (28.9 instead of 11.06). An increased interlayer coupling was also observed for thin films of tetrapyrrodo-tetraazaporphyrins on alkali halide [100] surfaces with prefactors of up to 24.¹² Highly ordered films of divalent phthalocyanine derivatives carrying electron-withdrawing ligands in general seem to show a higher interlayer coupling when compared to unsubstituted trivalent phthalocyanines.

The square-lattice orientation of $F_{16}PcZn$ (Figure 8) turned out to be the stable modification established at elevated temperature. Spatially extended coupling leads to the observed strong splitting (high prefactor). The clear broadening and decrease in intensity as observed in the temperature dependence of the absorption at 820 nm (Figure 5) shows, however, that this coupling is based on rather weak van der Waals interactions of the molecules. At lower temperature, intramolecular vibrations as well as vibrations of the whole molecules are smaller in amplitude leading to a smaller mobility of the molecules on the lattice sites. This smaller mobility leads to a well-defined electronic interaction at lower temperature which is weakened (smaller splitting) and partly lost (decrease in intensity) at increasing temperature. A decrease in intensity of the absorption band at 820 nm had also been observed in spectroelectrochemical experiments at $F_{16}PcZn$.³³ Reduction of the film had to be accompanied by the intercalation of cations at the expense of loosing this weak head-to-tail interaction of the molecules. This change was irreversible even after the ions had left the film after reversal of the potential. It is thereby confirmed that the band at 820 nm is a consequence of a rather extended coupling of the electronic transition vertical to the layer depicted in Figure 8 which is based, however, on a rather weak van der Waals interaction between the layers. This interpretation would also explain why we found a much more pronounced dependence on temperature in the red-shifted part of the spectrum as compared to the blue-shifted part.

Structure of MePTCDI Thin Films. For MePTCDI, more subtle changes in optical spectra have been observed during film growth, indicating significantly smaller changes in intermolecular orientation. A face-centered monoclinic crystal structure with two molecules per unit cell has been published,³⁴ and a representation of its b - c plane is given in Figure 8b.

An arrangement close to a parallel geometry is seen between the molecules along the c axis in the b - c plane at a distance of 1.46 nm and also between the molecules along the a axis between adjacent layers at a spacing of 0.39 nm. Due to the inverse cubic dependence of the splitting energy on dipole distance the interactions between molecules along the a axis

are about 20 times stronger than the interaction between molecules along the c axis. The main contribution to the blue-shifted band will therefore consist of interactions in the direction of the a axis of the crystal. This band is least influenced by a change in temperature, and the close proximity of molecules seems to be rather favorable to be preserved at all temperatures investigated; the interaction within the stack is kept basically constant.

The band furthest shifted to the red would have to be caused by a head-to-tail arrangement of molecules. Molecules along the b axis at a distance of 1.56 nm are placed close to this geometry. It seems to be this interaction which is again affected most significantly by changes in temperature and hence mobility of the molecules on their lattice sites. These transitions are electronically strongly coupled but based on very weak van der Waals forces leading to the strong temperature dependence. With decreasing temperature, the red shifted bands become considerably narrower and are shifted more strongly to lower energy, indicating a higher degree of order and a closer proximity of the molecules in the b - c plane due to a decrease of thermal motion especially in directions perpendicular to the a direction. MePTCDI can be looked at as a bundle of strongly bound, rigid, and highly ordered stacks of molecules (in the a direction) which are weakly bound among each other (in the b - c plane) and therefore show thermal motion especially in a transversal mode.

During the growth of films it is seen that the interactions along the a axis are established first, as the strongly blue-shifted band clearly dominates the spectra (Figure 7a) of thin films, before the red-shifted portion or the band at 485 nm has gained detailed structure. If the film growth starts from molecules oriented parallel to the substrate surface, as generally observed for PTCDA and related molecules,³ the stacks would be oriented perpendicular to the substrate surface and growth would predominantly occur in that direction. A formation of islands rather than a closed layer is thereby explained and was found in our conductivity measurements at MePTCDI during film growth (Figure 1b). Consistently a constant bulk spectrum was observed from a thickness of about 12 nm (Figure 7a) after first conductive pathways already were detected at about 10 nm.

Conclusions

Measurements of the electrical conductivity during film growth of molecular semiconductors provide good insight into the long-range properties and hence growth mode of films if the experiments are performed in situ and at a sensitivity which is sufficient to even detect conduction in monolayers. A surprisingly high conductivity could thus be determined for films of F₁₆PcZn of about monolayer thickness on glass. On top of this initially formed layer, islands were formed (Stranski-Krastanov growth) as seen in a decrease of conductivity. MePTCDI on the other hand grew in islands from the beginning (Volmer-Weber growth) that only allowed charge transport starting at considerably higher average film thickness. MePTCDI can thus be looked at as a typical example of island growth as observed for most organic films.

This strongly contrasting behavior in film growth was found to be caused by differences in crystal structures of the films as observed in optical absorption measurements during the growth of thin films. Such experiments could be performed in situ and hence represent a valuable tool to discuss structural order of the films in addition to experiments based on diffraction. Relative molecular positions within the films can be obtained in combination with model calculations since chromophore coupling is closely related to the relative intermolecular arrangement.

An increase in film temperatures during optical measurements of stable modifications of the films showed a clear broadening of peaks and a decrease of the dipole splitting energy characteristic for an increase of the mobility on the individual lattice sites as well as an increase in the average distance of chromophores. Substrate temperature during film growth proved to strongly influence the relative orientation of molecular lattice positions in F₁₆PcZn. A subsequent annealing of films also changed the crystal structure of films irreversibly. A significant mobility of molecules on the surface is thereby indicated as well as a rather high flexibility of F₁₆PcZn toward different intermolecular arrangements in the solid state.

After contact with O₂ or air no changes from the spectra in a vacuum and a stable optical absorption behavior was observed for all films in the present experiments. This finding confirmed our previous interpretation in which the changes as observed in electrical conductivity and excimer emission intensity were attributed to reactions with dopant impurities in the film and hence changes in the redox equilibrium within the film rather than to O₂-induced changes in crystal structure and hence changes in chromophore interaction.^{14,18,35,36} Only a small number of molecules was expected to participate in such reactions and only experiments specifically probing charged species at higher sensitivity via charge carrier generation or quenching of the excited states were influenced significantly but changes below the percent region did not interfere with the present measurements of the optical absorption.

Acknowledgment. The authors are grateful to DFG (Ja 346/12-1, Schl 340/3-1,2) and the State of Bremen (Senator für Bildung: MATEC, doctorand stipend funds) as well as SCAT (Japanese Ministry of Posts and Telecommunications) for financial support. At the University of Bremen we thank D. Wöhrle for many fruitful discussions, G. Schnurpfeil for providing C₁₆PTCDI, and the team of the machine shop for constructing parts of the experiments. We thank W.-D. Stohrer and M. Glodde (University of Bremen) as well as S. Mashiko and H. Suzuki (KARC, Kobe, Japan) for sharing parts of their equipment with us and participating in helpful discussions.

References and Notes

- (1) Law, K.-Y. *Chem. Rev.* **1993**, 93, 449.
- (2) Schmidt, A.; Chau, L.-K.; Back, A.; Armstrong, N. R. In *Phthalocyanines Properties and Applications*; Leznoff, C. C., Lever, A. B. P., Eds.; VCH: New York, 1996; Vol. 4.
- (3) Forrest, S. R. *Chem. Rev.* **1997**, 57, 1793.
- (4) Schmidt, A.; Schlaf, R.; Louder, D.; Chau, L.-K.; Chen, S.-Y.; Fritz, T.; Lawrence, M. F.; Parkinson, B.; Armstrong, N. R. *Chem. Mater.* **1995**, 7, 2127.
- (5) Assour, J. M. *J. Phys. Chem.* **1965**, 69, 2295.
- (6) Mindorff, M. S.; Brodie, D. E. *Can. J. Phys.* **1981**, 59, 249.
- (7) Hochstrasser, R. M.; Kasha, M. *Photochem. Photobiol.* **1964**, 3, 317.
- (8) Kasha, M.; Rawls, H. R.; Ashraf El-Bayoumi, M. *Pure Appl. Chem.* **1965**, 11, 371.
- (9) Czikkely, V.; Försterling, H. D.; Kuhn, H. *Chem. Phys. Lett.* **1970**, 6, 207.
- (10) Kasha, M. In *Spectroscopy of the Excited State*; Di Bartolo, B., Ed.; Plenum: New York, 1976.
- (11) Chau, L. K.; England, C. D.; Chen, S.; Armstrong, N. R. *J. Phys. Chem.* **1993**, 97, 2699.
- (12) Schlettwein, D.; Tada, H.; Mashiko, S. *Thin Solid Films* **1998**, 331, 117.
- (13) Gomez, U.; Leonhardt, M.; Port, H.; Wolf, H. C. *Chem. Phys. Lett.* **1997**, 268, 1.
- (14) Schlettwein, D.; Back, A.; Schilling, B.; Fritz, T.; Armstrong, N. R. *Chem. Mater.* **1998**, 10, 601.
- (15) Birks, J. B. *Photophysics of Aromatic Molecules*; Wiley: New York, 1970.
- (16) Bao, Z.; Lovinger, A. J.; Brown, J. J. *Am. Chem. Soc.* **1998**, 120, 207.

- (17) Hiller, S.; Schlettwein, D.; Armstrong, N. R.; Wöhrle, D. *J. Mater. Chem.* **1998**, 8, 945.
- (18) Meyer, J.-P.; Schlettwein, D. *Adv. Mater. Opt. Electron.* **1997**, 6, 239.
- (19) Akers, K.; Aroca, R.; Hor, A. M.; Loutfy, R. O. *Spectrochim. Acta* **1988**, 44A, 1129.
- (20) Kawato, S.; Hayashi, K.; Horiuchi, T.; Matsushige, K. *Mol. Cryst. Liq. Cryst.* **1996**, 280, 247.
- (21) Mizuguchi, J.; Rihs, G.; Karfunkel, H. R. *J. Phys. Chem.* **1995**, 99, 16217.
- (22) Gouterman, M.; Holten, D.; Lieberman, E. *Chem. Phys.* **1977**, 25, 139.
- (23) Siggel, U.; Bindig, U.; Endisch, C.; Komatsu, T.; Tsuchida, E.; Voigt, J.; Fuhrhop, J.-H. *Ber. Bunsen-Ges. Phys. Chem.* **1996**, 100, 2070.
- (24) Graser, F.; Hädicke, E. *Liebigs Ann. Chem.* **1980**, **1994**, **1984**, 483.
- (25) Graser, F.; Hädicke, E. *Acta Crystallogr.* **1986**, C42, 189, 195.
- (26) Klebe, G.; Graser, F.; Hädicke, E.; Berndt, F. *Acta Crystallogr.* **1989**, B45, 69.
- (27) Kazmaier, P. M.; Hoffman, R. *J. Am. Chem. Soc.* **1994**, 71, 9684.
- (28) Burgdorff, C.; Löhmansröben, H.-G.; Reisfeld, R. *Chem. Phys. Lett.* **1992**, 197, 358.
- (29) Rademacher, A.; Märkle, S.; Langhals, H. *Chem. Ber.* **1982**, 115, 2927.
- (30) Langhals, H.; Demmig, S.; Huber, H. *Spectrochim. Acta* **1988**, 11, 1189.
- (31) Hochstrasser, R. M. *J. Chem. Phys.* **1964**, 40, 2559.
- (32) Hiller, S. Diplomarbeit, Universität Bremen, 1995.
- (33) Hesse, K.; Schlettwein, D. *J. Electroanal. Chem.*, submitted.
- (34) Cambridge Structural Database, Cambridge Crystallographic Data Centre, Cambridge, U.K.
- (35) Schlettwein, D.; Armstrong, N. R.; Lee, P. A.; Nebesny, K. W. *Mol. Cryst. Liq. Cryst.* **1994**, 253, 161.
- (36) Schlettwein, D.; Armstrong, N. R. *J. Phys. Chem.* **1994**, 98, 11771.